

Chapter 2

Radar Fundamentals

The abbreviation *radar* stands for “radio detection and ranging”. It designates a radio technology for the determination of distances to remote stationary or moving objects. This chapter intends to give a brief overview about radar techniques [1].

2.1 Radar Equation

The radar principle is based on the properties of electromagnetic waves and its characteristic reflection at different materials. Thereby, a radio signal of wavelength λ is transmitted. Based on the reflected and received signal response conclusions regarding direction, distance, and relative velocity of the reflecting target can be drawn. The received signal strength of the target can be calculated after the radar equation:

$$P_r = \frac{P_t G_t A_r \sigma_S}{(4\pi)^2 R^4} \quad \text{with} \quad A_r = \frac{G_r \lambda^2}{4\pi}. \quad (2.1)$$

In the above expression, P_r denotes the received signal strength, while P_t represents the transmitted signal power. The antenna is characterized by its transmit and receive antenna gain G_t and G_r as well as the corresponding effective aperture A_r of the receiving antenna. σ_S is the scattering cross section of the reflecting target which is located at the distance R . The received signal strength degrades with a power of 4. This is in contrast to general communication systems which employ bidirectional transmission, leading to a much higher degradation in power levels. Therefore, the radar receiver has to provide a high sensitivity and dynamic range in order to cover a wide range of target distances.

2.2 Antenna Concepts

One can distinguish between mono- and bistatic radar architectures. These differ in the design of the transmit and receive antennas. Bistatic radar devices possess spatially separated antennas for the transmit (TX) and receive (RX) path. Figure 2.1 shows a schematic diagram of a bistatic radar architecture [2].

In a monostatic radar architecture a single antenna performs both the transmission and reception of the radar signal. Figure 2.2 shows a schematic diagram of a monostatic radar transceiver. The transmitted and received signals are separated through a circulator. Signals generated in the transmitter are passed directly to the antenna, while received signals from the antenna are routed to the receiver part. An ideal circulator theoretically provides infinite isolation between the transmit and receive path. Nevertheless, the isolation of millimeter-wave circulators over a certain bandwidth is limited and coupling effects have to be accounted for.

2.3 Carrier Modulation

2.3.1 Pulse-Doppler Radar

The distance from a target to the radar system can be determined by measuring the propagation delay between the transmitted and received signal. Figure 2.3 shows a block diagram of a pulse-doppler radar architecture. The oscillator generates a radio

Fig. 2.1 Schematic diagram of a bistatic radar architecture consisting of spatially separated radar transmitter and receiver with dedicated antennas

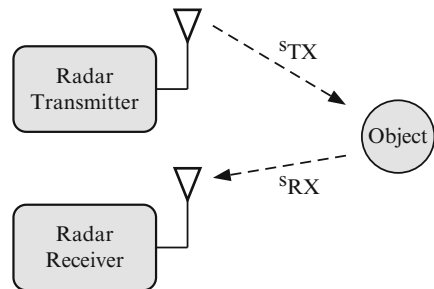
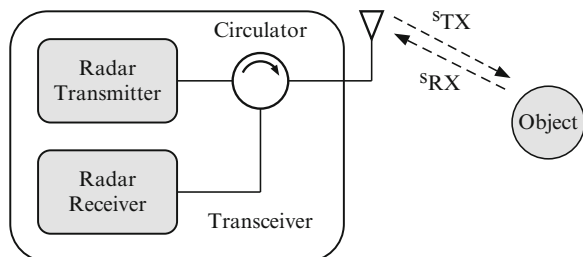


Fig. 2.2 Schematic diagram of a monostatic radar architecture consisting of transmitter, receiver, and a circulator for signal splitting at the antenna



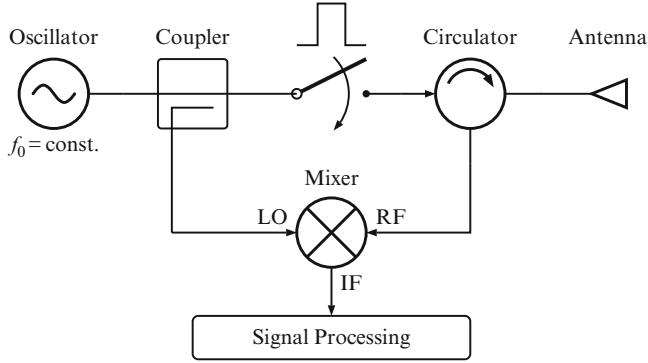


Fig. 2.3 Block diagram of a pulse-doppler radar transceiver architecture

signal at the constant frequency f_0 that is converted into a continuous pulse train by a pulse-shaping device and transmitted via the antenna. The incoming signal is mixed with the local oscillator (LO) signal and subsequently processed in the baseband.

If the propagation speed c of the electromagnetic wave in the medium is known, one can calculate the distance R between the obstacle and the radar system via the round trip propagation delay Δt of the impulse by (2.2). The radio wave propagation can be derived from the vacuum speed of light c_0 and material permittivity ϵ_r .

$$R = \frac{c\Delta t}{2} \quad \text{with} \quad c \approx \frac{c_0}{\sqrt{\epsilon_r}} \quad (2.2)$$

In addition to the above determination of the range to the target, the relative velocity of the object with respect to the radar system can be derived from the Doppler shift of the received signal frequency f_i . Equation 2.3 gives the relationship between relative velocity v_r and the Doppler frequency shift $f_d = f_i - f_0$.

$$v_r = \frac{cf_d}{2f_0} \quad \text{for} \quad v \ll c \quad (2.3)$$

The Doppler shift describes the shift of frequency caused by motion of the target with respect to the signal source. Depending on the direction of movement the shift is of positive value for objects approaching the signal source and takes a negative value for targets moving away from the radar transmitter.

Figure 2.4 shows the transmitted (a) and incoming (b) signals in a pulse-radar system. It possesses a maximum range which is defined by the pulse repetition rate T_P of the transmitter. The maximum unambiguous range R_{\max} is given by

$$R_{\max} = \frac{cT_P}{2}. \quad (2.4)$$

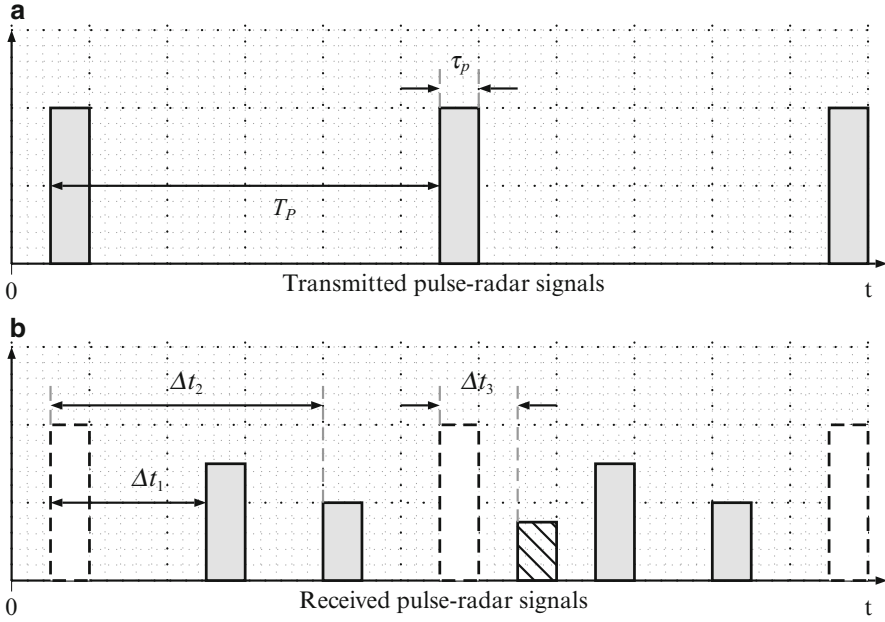


Fig. 2.4 Time dependent behavior of transmitted (a) and received (b) signals in a pulse-radar system; pulse repetition rate T_P , pulse width τ_p , propagation delay Δt

It defines the longest range a pulse can travel from the transmitter to the receiver before the next pulse is emitted. Violation of the above leads to the appearance of ghost targets as shown in Fig. 2.4b. In case the system receives an echo from a prior pulse after the following pulse has been transmitted, the distance to the target is falsely calculated to be Δt_3 instead of the actual range $T_P + \Delta t_3$. The range resolution of a pulse-radar dependent upon the pulse width τ_p is given as

$$\delta_r = \frac{c \tau_p}{2} \approx \frac{c}{2B}. \quad (2.5)$$

Two different targets can only be distinguished from each other as long as their individual backscattered pulse responses do not overlap and become blurred. The range resolution can be related to the inverse of the pulse bandwidth B by (2.5).

2.3.2 Frequency Modulated Continuous-Wave Radar

Unmodulated continuous-wave (CW) radars transmit a signal with constant frequency. The lack of modulation of the source only allows for determination of the relative target velocity via the Doppler shift. Frequency modulated continuous-wave

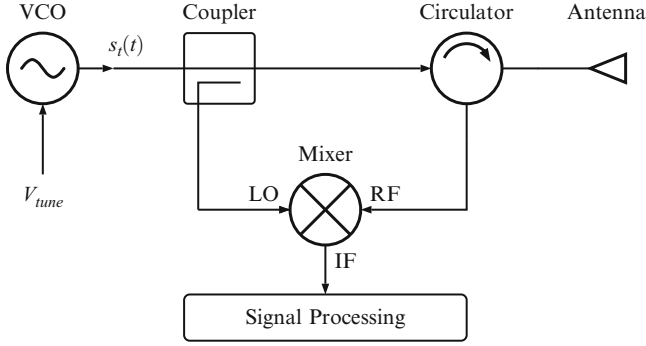


Fig. 2.5 Block diagram of a direct-conversion FMCW radar transceiver architecture

(FMCW) radar systems employ frequency modulation at the signal source to enable propagation delay measurements for determination of the distance to the target. Figure 2.5 shows a block diagram of an FMCW radar transceiver.

A voltage-controlled oscillator (VCO) forms the signal source that is modulated as a linear frequency ramp by changing the tuning voltage V_{tune} of the VCO. Equation 2.6 gives the mathematical expression for a frequency modulation that uses up- and down-chirps of equal length $T_P/2$ and bandwidth B .

$$f_t(t) = f_0 + kt \quad \text{with} \quad k = \frac{2B}{T_P} \quad (2.6)$$

The above modulation scheme yields a transmitted signal s_t of the form

$$s_t(t) = A_t \cos(2\pi f_t(t)t) \quad (2.7)$$

$$= A_t \cos(2\pi f_0 t + 2\pi k t^2). \quad (2.8)$$

A fraction of the signal is coupled to the receive mixer to act as the LO reference, while the other part is transmitted through the antenna. The backscattered signal

$$s_r(t - \Delta t) = A_r \cos(2\pi(f_0 + f_d)(t - \Delta t) + 2\pi k(t - \Delta t)^2) \quad (2.9)$$

with the propagation delay Δt and a Doppler shift f_d is received and translated into the baseband by means of a down-conversion mixer. Subsequently the intermediate frequency (IF) signal is digitized and the determination of target range and velocity is performed through a fast Fourier transformation (FFT).

Figure 2.6a shows the variation in frequency versus time for the transmitted and received signal. The VCO generates an up- and down-chirp of bandwidth B within a modulation period T_P . After transmission the reflected signal is received with a propagation delay Δt . If the target exhibits a relative velocity to the transmitter

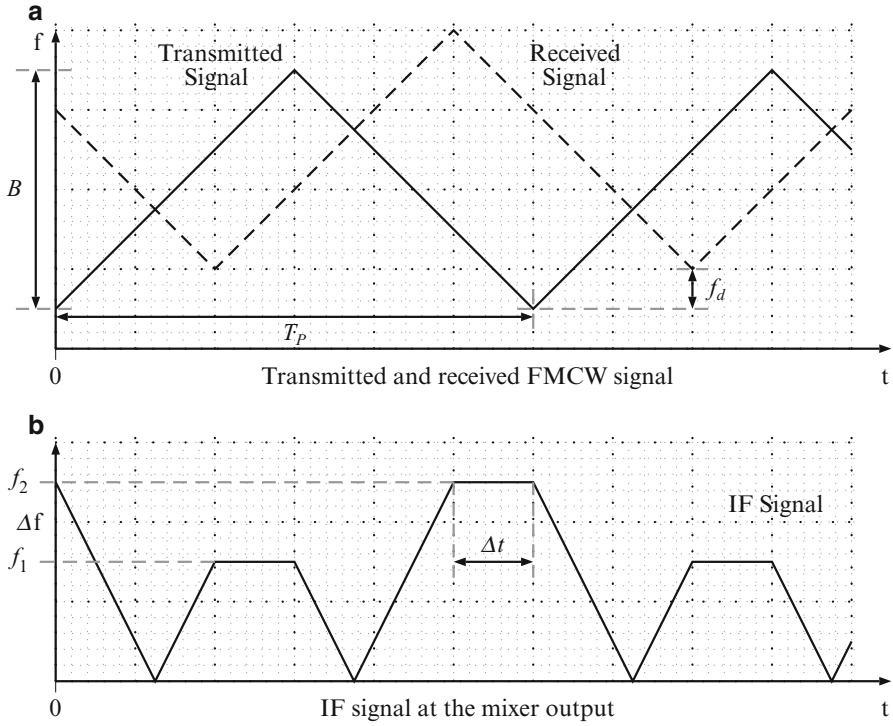


Fig. 2.6 Time dependent behavior of transmitted and received (a) and IF signal (b) of an FMCW radar system; propagation delay Δt , Doppler shift f_d , bandwidth B

the frequency of the received signal is shifted by f_d . The resulting IF signal is depicted in Fig. 2.6b. It represents the absolute of the frequency difference between the transmit and receive signal. Based on the two different IF frequencies f_1 and f_2 one can obtain the range R and relative velocity v_r of the target through

$$R = \frac{c T_p}{2B} \frac{f_1 + f_2}{2} \quad (2.10)$$

$$v_r = \frac{c}{2f_c} \frac{f_1 - f_2}{2}. \quad (2.11)$$

Furthermore, the range resolution δ_r of an FMCW radar system is given by

$$\delta_r = \frac{c}{2B}. \quad (2.12)$$

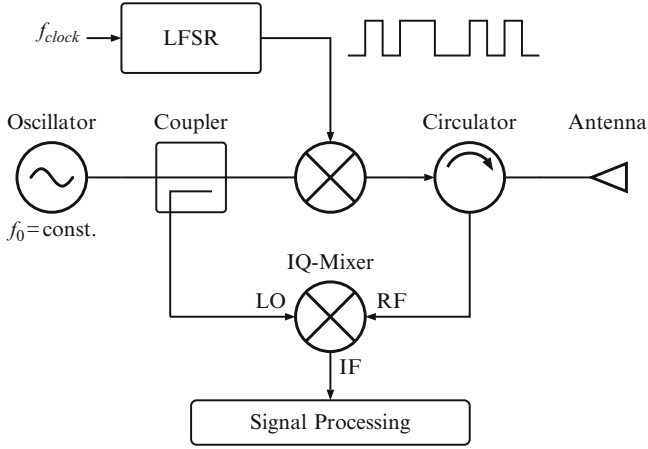


Fig. 2.7 Block diagram of a pseudo-noise modulated radar transceiver architecture

2.3.3 Pseudo-Noise Modulated Continuous-Wave Radar

In contrast to pulse-radar systems, where energy is transmitted in a short time period, the method of pulse compression allows to replace a pulse waveform by spread spectrum signals that distribute their energy over a long time. This can be achieved by phase or frequency modulation of the carrier with a pseudo-random binary sequence (PRBS) to reduce the peak power of the radar system [3]. A maximum length binary sequence (M-sequence) is a special type of PRBS signal that can be generated through a linear feedback shift register (LFSR). An N -stage shift register can generate a pseudo-random code of the length $2^N - 1$. Figure 2.7 shows a diagram of a PRBS modulated radar system.

The linear feedback shift register generates an M-sequence that is up-converted onto the carrier frequency f_0 by a biphase modulator [4]. The resulting double-sideband spectrum is transmitted via the antenna. To avoid loss of information, a quadrature down-conversion mixer is implemented in the receiver path, which translates the signal into the baseband [5]. The signal processing unit performs correlation of the IF signal and the reference PRBS code in the digital domain.

Figure 2.8 shows the exemplary time shape of a fourth-order M-sequence [6]. The pseudo random sequence is periodic with a period of T_p , that is related to the chip duration t_c and the number of bits N by

$$T_p = Nt_c. \quad (2.13)$$

The power spectrum of an M-sequence is the Fourier transform of its autocorrelation function, which is approximately equal to a single rectangular segment. This results in a line spectrum as shown in Fig. 2.9 with an envelope shape $S(f)$ determined by a sinc^2 function according to (2.14). The spacing between the

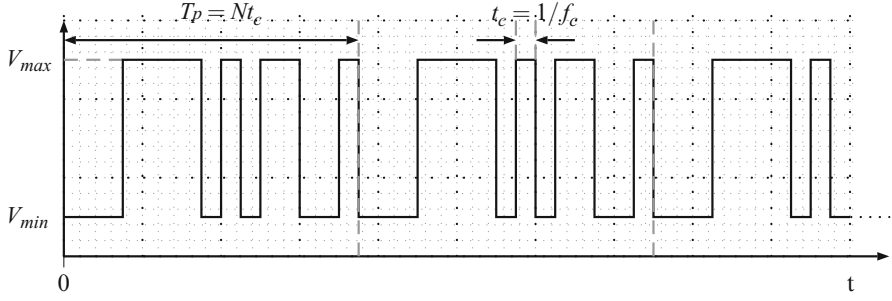


Fig. 2.8 Time shape of a fourth-order M-sequence; pseudo random sequence period T_p , number of bits N , chip duration t_c , and bandwidth f_c

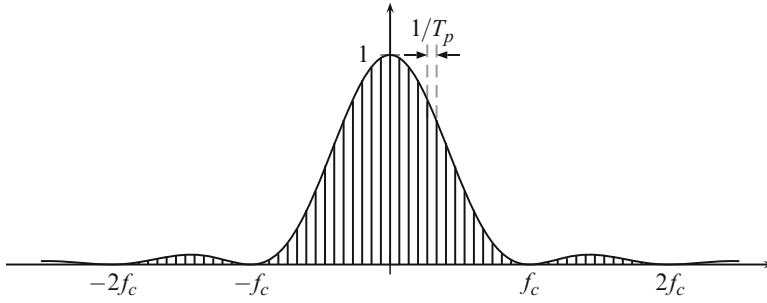


Fig. 2.9 Representation of a fourth-order M-sequence in the frequency domain; pseudo random sequence period T_p , chip duration t_c , and bandwidth f_c

individual lines depends on the period T_p of the M-sequence.

$$S(f) = \text{sinc}^2(\pi f t_c) = \frac{\sin^2(\pi f t_c)}{(\pi f t_c)^2} \quad (2.14)$$

A direct relationship between the bandwidth f_c of the PRBS code and the minimum achievable range resolution δ_r exists:

$$\delta_r = \frac{c}{2f_c}, \quad (2.15)$$

and the supported unambiguous range R_{\max} is calculated to

$$R_{\max} = \frac{c T_p}{2} = \frac{c N}{2f_c}. \quad (2.16)$$

In order to achieve a low range resolution δ_r and at the same time support a large unambiguous range R_{\max} , the chip duration t_c is required to remain small while the bit-length N of the M-sequence has to be sufficiently large. Moreover, in ranging systems based on spread spectrum techniques, a large value of N is necessary to improve the autocorrelation function of the sequence which lowers the cross-correlation function. This allows the system to discriminate among other spread spectrum signals, e.g. radar transmitters of other traffic participants [7].

2.4 Automotive Radar

In Europe alone about 1.3 million traffic accidents cause more than 41,000 fatalities and an economical damage of more than 200 billion Euros per year. Human error is involved in over 90% of the overall accidents. The introduction of preventive safety applications into the car can avoid the above errors by e.g. helping the driver to maintain a safe speed and distance, keep within the lane, and prevent overtaking in critical situations. Figure 2.10 depicts a number of different technologies that are used in active safety systems to monitor the surrounding environment of a vehicle.

The first generation of driver assistance systems only featured comfort functions. Adaptive Cruise Control (ACC) based on 77 GHz Long Range Radar (LRR) automatically adjusts the driving speed of the vehicle to maintain a constant distance to the car ahead. Parking aid and parking slot measurement based on ultrasound and 24 GHz Short Range Radar (SRR) support the driver during the parking process.

In the current generation, passive safety features are employed. Lane change assistance and blind spot detection systems warn the driver if other vehicles would be critical in case of a lane changing maneuver. Pre-crash sensing and collision warning systems alert the driver of an imminent critical situation, pre-regulate the necessary braking pressure and prepare safety measures to mitigate the results of a

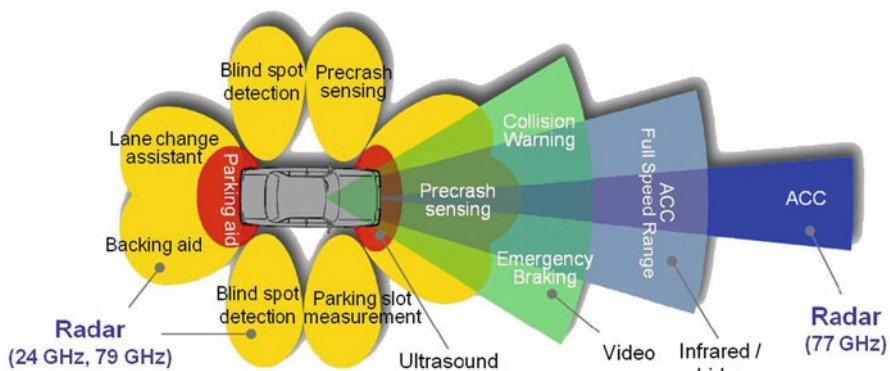


Fig. 2.10 Surrounding field monitoring technologies for driver assistance systems

Table 2.1 Comparison of different automotive radar sensor classifications

	Long range radar	Mid range radar	Short range radar
Frequency band	77 GHz	79 GHz	79 GHz
Max. output power EIRP	+55 dBm	−9 dBm/MHz	−9 dBm/MHz
Bandwidth	600 MHz	600 MHz	4 GHz
Distance range	10–250 m	1–100 m	0.15–30 m
Distance resolution	0.5 m	0.5 m	0.1 m
Speed resolution	0.1 m/s	0.1 m/s	0.1 m/s
Angular accuracy	0.1°	0.5°	1°
3 dB Beamwidth Azimuth	±15°	±40°	±80°
3 dB Beamwidth elevation	±5°	±5°	±10°

Table 2.2 Comparison of currently available automotive radar frequency bands

		24 GHz ISM ^a	24 GHz UWB ^a	77 GHz LRR	79 GHz SRR
Europe	Bandwidth	200 MHz	5 GHz ^b	1 GHz	4 GHz
	Power EIRP	+20 dBm	−41.3 dBm/MHz	+55 dBm	−9 dBm/MHz
USA	Bandwidth	100/250 MHz	7 GHz	1 GHz	Negotiations
	Power EIRP	+32.7/12.7 dBm	−41.3 dBm/MHz	+23 dBm	
Japan	Bandwidth	76 MHz	5 GHz	0.5 GHz	Planned
	Power EIRP	+10 dBm ^c	−41.3 dBm/MHz	+10 dBm ^c	

^aNot protected for automotive radar

^bOnly until 2013

^cTransmit power at antenna feed

possible collision. Future active safety systems will initiate an emergency brake if the sensor data indicates that a collision cannot be avoided. Additional rear sensors enable the determination of an optimum deceleration to avoid a potential collision with the following car [8].

In comparison to optical systems, e.g. video or lidar, radar based sensors can operate reliably under a variety of different environmental situations. They are robust against rough weather, e.g. rain, fog, or snow, as well as lighting conditions. Furthermore, radar sensors can be installed in the vehicle behind plastic radomes that are electromagnetically transparent to the radar signals, making them invisible in the exterior design of the car.

Table 2.1 shows a comparison between different automotive radar sensor classifications [9]. Long range radar sensors in the 76–77 GHz band operate over a distance range up to 200 m but require only a moderate distance resolution. Therefore, a bandwidth of only 200–600 MHz is sufficient, but a high angular resolution is necessary due to the narrow field of view. On the contrary, short range radar sensors possess a wide beamwidth in the azimuth to cover a large viewing area. The range accuracy requirements are below 10 cm which necessitates a bandwidth of 4 GHz.

Different frequency bands exist that are dedicated or can be used for automotive radar applications. Table 2.2 shows a comparison of the currently available frequency bands in the main markets. In Europe the 24 GHz UWB band has only

been temporarily allocated for short range applications. From 2013 the frequency regulation demands that new cars have to be equipped with 79 GHz short range radar sensors [10]. Similar allocations are planned in Japan and are currently under negotiation in the United States.

References

1. M. I. Skolnik, *Radar Handbook*, 3rd ed. McGraw-Hill, 2008.
2. N. J. Willis and H. D. Griffiths, *Advances in Bistatic Radar*. Scitech Pub, 2007.
3. B. Sewiolo, "Ultra-wideband transmitters based on M-sequences for high resolution radar and sensing applications," Ph.D. dissertation, Inst. for Electron. Eng., Univ. of Erlangen-Nuremberg, Erlangen, Germany, 2010.
4. S. Trotta, H. Knapp, D. Dibra, K. Aufinger, T. F. Meister, J. Böck, W. Simbürger, and A. L. Scholtz, "A 79 GHz SiGe-bipolar spread-spectrum TX for automotive radar," in *IEEE Int. Solid-State Circuits Conf. Dig. Tech. Papers*, San Francisco, CA, Feb. 2007, pp. 430–431.
5. B. Dehlink, H.-D. Wohlmuth, K. Aufinger, F. Weiss, and A. L. Scholtz, "An 80 GHz SiGe quadrature receiver frontend," in *IEEE Compound Semicond. Integr. Circuits Symp. Tech. Dig.*, San Antonio, TX, Nov. 2006, pp. 197–200.
6. D. J. Daniels, *Ground Penetrating Radar*, 2nd ed. The Institution of Engineering and Technology, 2004.
7. H.-J. Zepernick and A. Finger, *Pseudo Random Signal Processing - Theory and Application*. John Wiley & Sons, 2005.
8. H. L. Bloecher, J. Dickmann, and M. Andres, "Automotive active safety & comfort functions using radar," in *IEEE Int. Conf. Ultra-Wideband*, Vancouver, Canada, Sep. 2009, pp. 490–494.
9. M. Köhler, J. Hasch, F. Gumbmann, L.-P. Schmidt, J. Schür, and H. L. Bloecher, "Automotive radar operation considerations and concepts at frequencies beyond 100 GHz," in *Proc. Eur. Radar Conf. Workshop "Automotive Radar Sensors in the 76-81 GHz Frequency Range"*, Paris, France, Oct. 2010.
10. K. M. Strohm, H. L. Bloecher, R. Schneider, and J. Wenger, "Development of future short range radar technology," in *Proc. Eur. Radar Conf.*, Paris, France, Oct. 2005, pp. 165–168.

Millimeter-Wave Receiver Concepts for 77 GHz

Automotive Radar in Silicon-Germanium Technology

Kissinger, D.

2012, XIV, 111 p. 100 illus., 42 illus. in color., Softcover

ISBN: 978-1-4614-2289-1